

# The Impact of Inter-Pin Spatial Self-Shielding on Pin-Wise Reaction Rates

William Boyd, Benoit Forget, Kord Smith

Massachusetts Institute of Technology, Department of Nuclear Science and Engineering, 77 Massachusetts Avenue, Building 24, Cambridge, MA 02139, United States

---

## Abstract

**Keywords:** Whole-core neutron transport, multi-group cross-sections, spatial self-shielding, spatial homogenization

---

## 1. Introduction

Significant progress has been made in recent years to develop deterministic neutron transport-based tools for full-core reactor analysis [CITE: MPACT, nTracer, MPACT, Denovo, PROTEUS, TexasAM]. These efforts are motivated by the desire to obtain Monte Carlo-quality solutions with computationally efficient multi-group methods. The focal point for much of this work has been the implementation and analysis of parallel algorithms to make full-core analysis feasible on large computing machines [CITE]. However, much work remains to develop methods for multi-group cross section (MGXS) generation that enable multi-group transport codes to achieve sufficient predictive accuracy to complement (or replace) analysis with continuous energy Monte Carlo methods.

A two-pronged approach is needed to generate MGXS which enable Monte Carlo-quality solutions with multi-group methods. First, the approximation errors inherent to multi-group transport methods must be rigorously isolated and quantified by benchmarking multi-group transport with continuous energy Monte Carlo methods on fully-detailed heterogeneous benchmarks. These approximation errors may take on more (or less) relevance than they did for validation of the coarse-mesh multi-group diffusion-based codes used today. Second, the quantifiable results from these analyses should inform the development of solutions that rectify biases observed between multi-group and continuous energy transport methods.

This paper specifically investigates approximation error due to the effects of spatial self-shielding in Pressurized Water Reactors (PWRs) on multi-group cross sections. The effects of neighboring pins, control rod guide tubes, burnable poisons, water reflectors and the core baffle are each of interest in the context of spatial self-shielding. In particular, this paper quantifies the difference in the approximation error between simulations in which the same MGXS are used for each unique fuel pin *composition* (e.g., each fuel enrichment), and those in which unique MGXS are used in each *instance* of each fuel pin throughout a core geometry. The former approach does little to model spatial self-shielding effects beyond those accounted for by an infinite fuel pin lattice model, while the latter goes much further to resolve inter-pin spatial self-shielding effects, albeit at the expense of much larger MGXS libraries.

This work employs Monte Carlo (MC) neutron transport simulations to generate MGXS. Monte Carlo methods have increasingly been used to generate few group constants for coarse mesh diffusion, most notably by the Serpent MC code (Leppänen, 2013), and to a much lesser extent, for high-fidelity neutron transport methods (Redmond, 1997; Nelson, 2014; Cai, 2014; Boyd, 2016). The advantage of a MC-based approach is that all of the relevant physics are directly embedded into MGXS by weighting the continuous energy cross sections with a statistical proxy to the true neutron scalar flux. This paper replaces the traditional multi-step approach to MGXS generation with a single Monte Carlo eigenvalue calculation of the complete benchmark geometry to generate MGXS for each fuel pin instance. Furthermore, the same MC calculation is used to compute a reference solution to benchmark the approximate solution from a multi-group code and to quantify the significance of spatially self-shielded MGXS.

The content in this paper is organized as follows. The methodology used to generate MGXS is discussed in Sec. 2. The simulation tools for continuous energy Monte Carlo simulations with OpenMC, and deterministic multi-group calculations with OpenMOC, are discussed in Sec. 3. Two heterogeneous PWR benchmarks used are presented in Sec. 4 to evaluate the efficacy of the spatial self-shielding models in Sec. 5. The need for a new, flexible approach to spatial homogenization which appropriately captures spatial self-shielding effects with minimal computational expense is discussed in Sec. 6.

## 2. MGXS Generation

This paper uses Monte Carlo to generate MGXS for deterministic methods. The single-step framework used to generate MGXS from Monte Carlo is discussed in Sec. 2.1. The two pin-wise spatial homogenization schemes used to quantify approximation error due to inter-pin spatial self-shielding model are introduced in Sec. 2.2.

### 2.1. A Single-Step Framework

In general, MGXS generation schemes use a multi-step approach to decouple the energy, angular and spatial dimensions of the transport equation. The multi-step approach typically applies high-fidelity models of the energy self-shielding physics to low-fidelity geometric models of unique core components. The multi-step approach uses a combination of models

---

Email addresses: wboyd@mit.edu (William Boyd), bforget@mit.edu (Benoit Forget), kord@mit.edu (Kord Smith)

of varying complexity to optimize overall simulation speed with accuracy. However, this is often done at the expense of generality. For example, multi-step MGXS generation schemes do not typically model inter-assembly physics or the effect of reflectors and other core heterogeneities on the spatial distribution of the flux. Instead, geometric heuristics are often used to embed spatial self-shielding effects in MGXS for similarly shielded spatial zones (e.g., fuel pins with similar neighboring pins). The approximations to the energy and spatial variation of the flux introduce approximation error in full-core calculations and limit the core design parameter space for which multi-level schemes may be applied.

This work abandons the multi-step approach in favor of a single-step framework. Furthermore, this work employs Monte Carlo methods to generate MGXS since it presents a natural approach to replace engineering prescriptions to approximate the flux with a stochastic approximation of the exact flux. However, MC-based MGXS generation methods to date have retained the multi-step geometric framework to tabulate MGXS for individual reactor components – such as infinite fuel pins and/or assemblies – for subsequent use in full-core multi-group calculations. Although the use of MC within a multi-step framework eliminates the need to approximate the flux in energy, it does not account for spatial self-shielding effects throughout a reactor core.

This work takes an additional step and uses MC eigenvalue simulations of the complete heterogeneous geometry to simultaneously account for all energy and spatial effects in a single step. The single-step framework may be impractical for MGXS generation for industrial applications since it is constrained by the slow convergence rate of Monte Carlo tallies. Nevertheless, it allows for the rigorous quantification of approximation error due to spatial self-shielding models used to generate MGXS, which is the focal point of this paper.

## 2.2. Pin-wise Spatial Self-Shielding Models

This paper employs two different spatial homogenization schemes to model spatial self-shielding effects in MGXS. Although all spatial zones may experience spatial self-shielding, this chapter only models the impact of spatial self-shielding on MGXS in fissile regions. The null and degenerate spatial homogenization schemes are introduced in [Sec. 2.2.1](#) and [Sec. 2.2.2](#), respectively. These schemes model spatial self-shielding for each fuel pin with increasing granularity and complexity.

### 2.2.1. Null Spatial Homogenization

The *null* spatial homogenization scheme uses a single Monte Carlo calculation of the complete heterogeneous geometry to generate MGXS for each material. The spatially self-shielded flux is used to collapse the cross sections in each material with a unique isotopic composition. The null scheme does not account for spatial self-shielding effects experienced by different fuel pins filled by the same fuel composition, and instead averages these effects across the entire geometry. A single MGXS is employed in each instance of a material

zone, such as a fuel pin replicated many times throughout a benchmark geometry. The null scheme serves as the base case in this paper to illustrate the approximation error which results when inter-pin spatial self-shielding effects are neglected, even when the exact flux from Monte Carlo is used to collapse continuous energy cross sections.

### 2.2.2. Degenerate Spatial Homogenization

The *degenerate* spatial homogenization scheme accounts for spatial self-shielding effects experienced by each instance of each fuel pin throughout a heterogeneous geometry. Like the null scheme, a single MC calculation of the complete heterogeneous geometry is used to generate MGXS for all materials. Unlike the null scheme, the MGXS are tallied separately for each instance of fissile material zones. For example, if a heterogeneous benchmark includes  $N$  fuel pins, then  $N$  collections of MGXS are separately tabulated for each fuel pin instance. The degenerate scheme tallies different MGXS even if the isotopic compositions in the fuel pin instances are identical, since each instance may experience different spatial self-shielding effects and hence have different MGXS. The degenerate scheme demonstrates the reduction in approximation error between multi-group and continuous energy transport methods that can be achieved when inter-pin spatial self-shielding effects are sufficiently modeled in MGXS.

## 3. Simulation Tools

This work employed both continuous energy and multi-group neutron transport codes. The OpenMC Monte Carlo code ([Romano and Forget, 2013](#)) was generated multi-group cross sections and reference solutions as discussed in [Sec. 3.1](#). The MGXS generated by OpenMC were used by the OpenMOC code ([Boyd et al., 2014](#)) for deterministic multi-group transport calculations as highlighted in [Sec. 3.2](#).

### 3.1. Continuous Energy Calculations with OpenMC

The OpenMC continuous energy Monte Carlo (MC) code ([Romano and Forget, 2013](#)) was employed to generate multi-group cross sections, and reference eigenvalues and pin-wise fission and capture reaction rates. The `openmc.mgxs` Python module was used to tally multi-group cross sections in CASMO's seventy energy group structure ([Rhodes et al., 2006](#)) from a single eigenvalue calculation. The multi-group cross sections were calculated with OpenMC's distributed cell tally algorithm ([Lax et al., 2014](#)), which permits spatial tally zones across repeated cell instances. In particular, unique MGXS were computed for each fuel pin cell with distributed cell tallies ([Lax et al., 2014](#)) in the repeating lattice benchmarks described in [Sec. 4](#). The OpenMC simulations were performed with 1000 batches with  $10^6$  particle histories per batch for each benchmark. Stationarity of the fission source was obtained with 100 inactive batches for each benchmark.

The OpenMC simulations used the “iso-in-lab” feature to enforce isotropic in lab scattering. The “iso-in-lab” feature samples the outgoing neutron energy from the scattering laws

prescribed by the continuous energy cross section library, but the outgoing neutron direction of motion is sampled from an isotropic in lab distribution. Although isotropic in lab scattering is a poor approximation for LWRs, it eliminated scattering source anisotropy as one possible cause of approximation error between OpenMC and OpenMOC. This simplification made it possible to isolate the approximation error resulting from the spatial self-shielding model used to generate MGXS.

### 3.2. Multi-Group Calculations with OpenMOC

The OpenMOC code (Boyd et al., 2014) was employed to use the MGXS generated by OpenMC for deterministic multi-group calculations. The OpenMOC code is a 2D method of characteristics code designed for fixed source and eigenvalue neutron transport calculations. OpenMOC approximates the scattering source as isotropic in the lab coordinate system, and discretizes the geometry into flat source regions (FSRs) which approximate the neutron source as constant across each spatial zone. The OpenMOC eigenvalue and energy-integrated, pin-wise reaction rates were compared with the reference solution computed by OpenMC.

Each OpenMOC simulation used a characteristic track lay-down with 128 azimuthal angles and 0.05 cm spacing. All eigenvalue calculations were converged to  $10^{-5}$  on the root mean square of the energy-integrated fission source in each FSR. The Coarse Mesh Finite Difference (CMFD) acceleration scheme was employed on a pin-wise spatial mesh to reduce the number of iterations required to converge the fine-mesh transport calculations. The 70-group MGXS used for MOC were collapsed to a 14-group structure for CMFD to significantly improve the speed of the CMFD eigenvalue calculations.

## 4. Test Cases and Reference Results

This paper modeled two test cases derived from the Benchmark for Evaluation And Validation of Reactor Simulations (BEAVRS) PWR model (Horelik et al., 2013). Each test case includes heterogeneous features – and corresponding spatial self-shielding effects – in order to understand their implications for accurate pin-wise MGXS generation. Although BEAVRS is an axially heterogeneous 3D core model, both benchmarks were fabricated in 2D due to the geometric constraints in OpenMOC. The impact of fuel enrichment, control rod guide tubes (CRGTs), burnable poisons (BPs), inter-assembly currents and water reflectors is considered. The geometric and material specifications for the two test cases are summarized in Sec. 4.1. The reference results computed with OpenMC are discussed in Sec. 4.2.

### 4.1. Benchmark Configurations

The two test cases were comprised of materials from the BEAVRS model, including 1.6% and 3.1% enriched  $\text{UO}_2$  fuel, borated water<sup>1</sup>, zircaloy, helium, air, borosilicate glass and

stainless steel. The densities and isotopic compositions for each material are detailed in the BEAVRS specifications (Horelik et al., 2013). Each material was modeled with cross sections from the ENDF/B-VII.1 continuous energy cross section library (X-5 Monte Carlo Team, 2003) evaluated at 600K for hot zero power conditions.

The first benchmark was a single fuel assembly with an array of 264 fuel pins of 1.6% enriched  $\text{UO}_2$  fuel with zircaloy cladding and a helium gap. The assembly included 24 CRGTs filled by borated water and surrounded by zircaloy cladding, and a central instrument tube filled with air surrounded by two zircaloy tubes separated by borated water. The intra-pin grid spacer and grid sleeve separating each assembly in the BEAVRS model were not included in the assembly benchmark. The assembly was modeled with reflective boundary conditions. The fuel assembly benchmark is illustrated for null and degenerate spatial homogenization in Fig. 1.

The second benchmark was constructed as a  $2 \times 2$  colorset of two fuel assemblies extracted from the BEAVRS model. The top-left and bottom-right fuel assemblies in the colorset were of the same enrichment and configuration as the first benchmark configuration. The top-right and bottom-left fuel assemblies included 264 fuel pins of 3.1% enriched  $\text{UO}_2$  fuel, 20 CRGTs and a central instrument tube. In addition, the two 3.1% enriched assemblies included four BPs consisting of eight layers of air, steel, borosilicate glass and zircaloy. The colorset was surrounded by a water reflector on the bottom and right that was of the same width as a fuel assembly. The colorset was modeled with reflective boundaries on the top and left and vacuum boundaries on the bottom and right. The colorset benchmark is illustrated for null and degenerate spatial homogenization in Fig. 1.

Flat source region spatial discretization meshes were applied to both benchmarks for the OpenMOC simulations as shown in Fig. 2. The  $\text{UO}_2$  fuel was subdivided into five equal volume radial rings, while ten radial rings were employed in the water-filled CRGTs and instrument tubes. The borosilicate glass and borated water material zones filling the BPs were each discretized into five equal volume radial rings. Five equally spaced rings were used in the moderator zones surrounding each pin. Eight equal angle subdivisions were used in all pin cell material zones. The 13.85824 cm of water reflector nearest the fuel assemblies in the colorset benchmark was discretized in a  $0.125984 \text{ cm} \times 0.125984 \text{ cm}$  rectilinear mesh, equivalent to a  $10 \times 10$  mesh in each pin. The 7.55904 cm of reflector furthest from the fuel assemblies was discretized in a  $1.25984 \text{ cm} \times 1.25984 \text{ cm}$  pin-wise mesh.

### 4.2. Verification Metrics

A series of OpenMC simulations were used to calculate reference eigenvalues, pin-wise fission rates, and pin-wise U-238 capture rates for both benchmarks. The reference solutions were computed with 100 inactive and 900 active batches of  $10^7$  particle histories per batch. The reference eigenvalues are listed in Tab. 1. The OpenMC “combined” eigenvalue estimator is reported along with the associated 1-sigma uncertainty of one pcm for both test cases.

<sup>1</sup>The water consisted of 975 parts per million (ppm) boron.



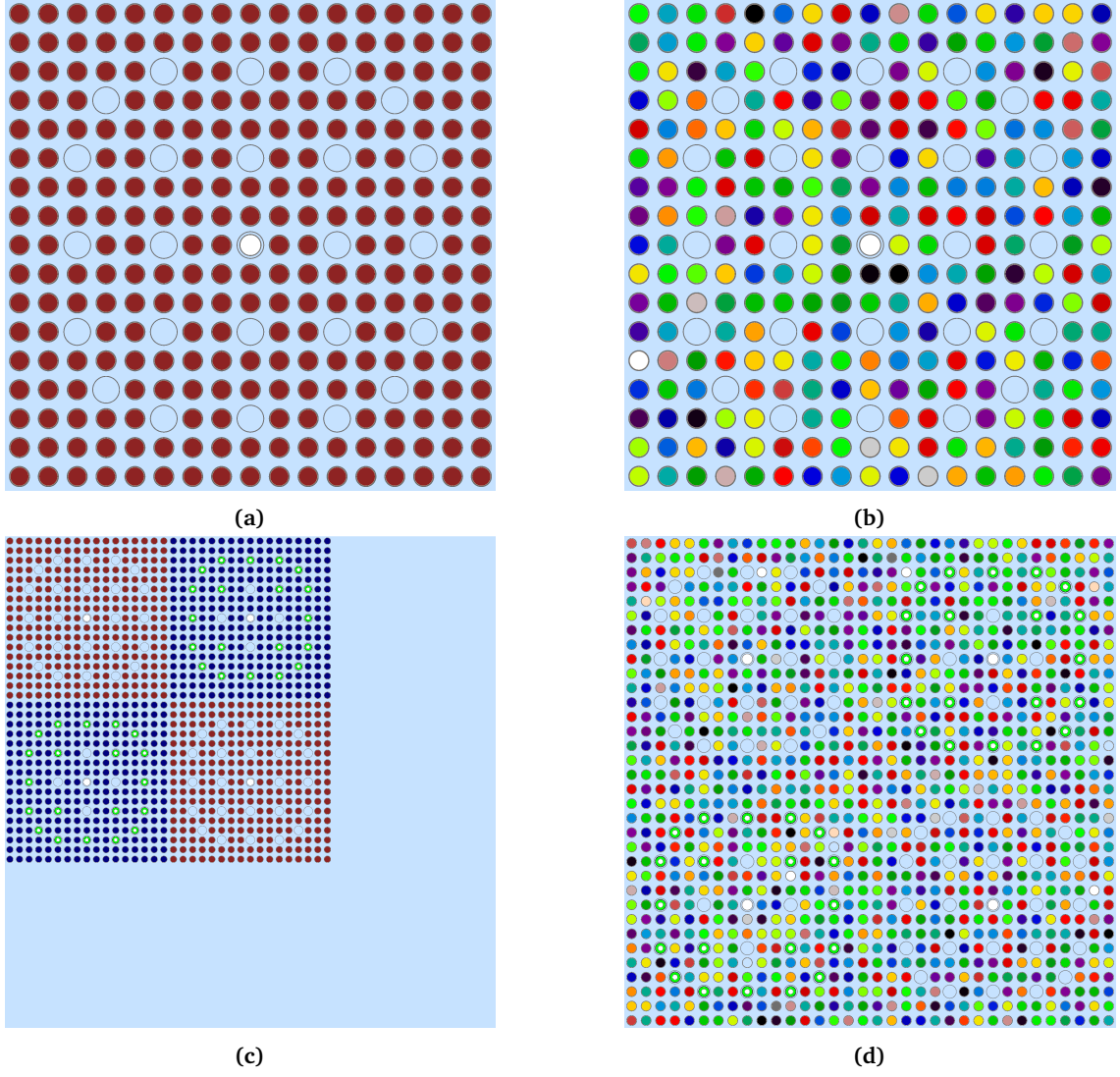


**Figure 1.** OpenMOC materials for the assembly (a) – (b) and colorset (c) – (d) benchmarks with null and degenerate homogenization, respectively.

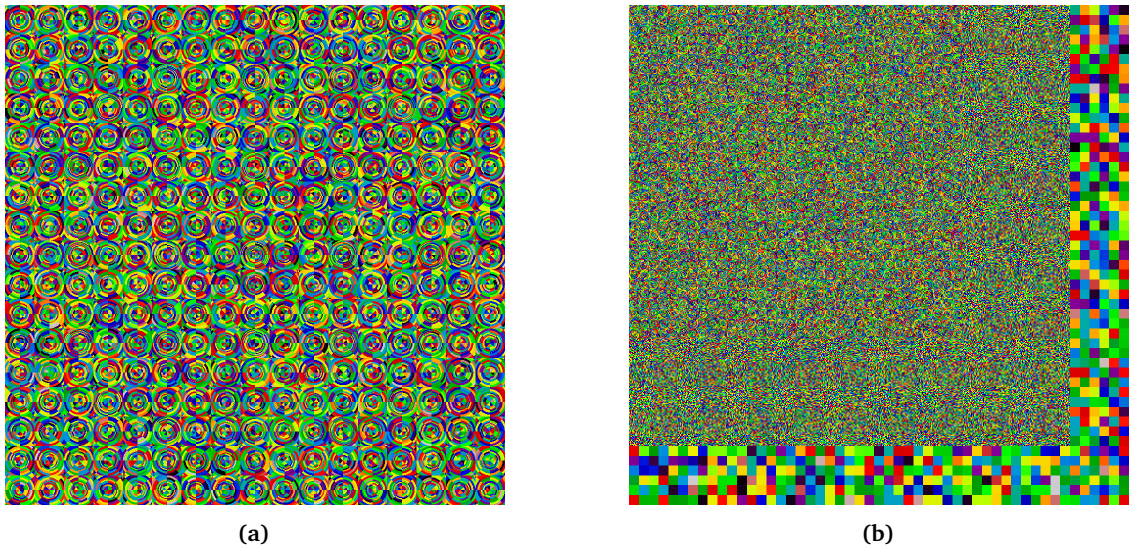


**Figure 2.** FSRs for the assembly (a) and colorset (b) benchmarks.

**Table 1.** Reference OpenMC eigenvalues for each benchmark.

Assembly	Colorset
$0.99326 \pm 0.00001$	$0.94574 \pm 0.00001$

The reference energy-integrated fission and U-238 capture rate spatial distributions were computed using rectilinear, pin-wise tally meshes in OpenMC and are shown in Fig. 3. The reaction rates were volume-integrated across each fuel pin. The fission rates include fission from only U-235 and U-238 for the fresh PWR UO<sub>2</sub> fuel. The reaction rates were normalized to the mean of all non-zero reaction rates in each benchmark. The reaction rates in the instrument tubes, CRGTs and BPs are all zero and are illustrated in white. The 1-sigma uncertainties are less than 0.08% in each pin for each benchmark.

As illustrated in the figures, the reaction rate distributions are strongly dependent on the spatially heterogeneous features in each benchmark. For example, the CRGTs provide additional moderation and increase the fission and U-238 capture rates in nearby fuel pins. The inclusion of BPs reduces the neutron population and therefore the reaction rates for the surrounding fuel pins. The presence of a reflector with a mixture of vacuum and reflective BCs induces a tilt in the reaction rates across the assemblies in the colorset.

Although spatial heterogeneities generally have similar effects on both fission and U-238 capture rates, there are a few important differences to note. The U-238 capture rates in the assemblies are more sensitive than the fission rates to the spatial self-shielding induced by moderation in CRGTs. In addition, the capture rates in the colorset are more smoothly varying at the inter-assembly and assembly-reflector interfaces than the fission rates.

## 5. Results

### 5.1. Eigenvalues

In the results that follow, the bias  $\Delta\rho$  compares the eigenvalue  $k_{eff}^{MOC}$  computed by OpenMOC to that of the reference eigenvalue  $k_{eff}^{MC}$  computed by OpenMC in units of pcm:

$$\Delta\rho = (k_{eff}^{MOC} - k_{eff}^{MC}) \times 10^5 \quad (1)$$

**Table 2.** OpenMOC eigenvalue bias  $\Delta\rho$ .

Benchmark	Null	Degenerate
Assembly	-161	-161
Colorset	-142	-132

### 5.2. Fission Rates

-add figures of spatial distribution of errors -can I reproduce these plots? Do I have the batchwise.h5 results stored on my external hard drive??? If so, I should customize them for only 70 groups

**Table 3.** OpenMOC fission rate percent relative errors.

Benchmark	Metric	Null	Degenerate
Assembly	Max	0.380	0.315
	Mean	0.074	0.079
Colorset	Max	0.764	0.602
	Mean	0.178	0.138

### 5.3. Capture Rates

-add figures of spatial distribution of errors

**Table 4.** OpenMOC U-238 capture rate percent relative errors.

Benchmark	Metric	Null	Degenerate
Assembly	Max	-1.101	0.386
	Mean	0.479	0.086
Colorset	Max	-1.969	-0.783
	Mean	0.478	0.165

## 6. Conclusions

### Acknowledgments

This work was supported by the Idaho National Laboratory and the National Science Foundation Graduate Research Fellowship Grant No. 1122374. This research made use of the resources of the High Performance Computing Center at Idaho National Laboratory, which is supported by the Office of Nuclear Energy of the U.S. Department of Energy and the Nuclear Science User Facilities under Contract No. DE-AC07-05ID14517.

### References

- Boyd, W., Forget, B., Smith, K., 2015. OpenCG: A Combinatorial Geometry Modeling Tool for Data Processing and Code Verification. In: Int'l Conf. on Mathematics and Computational Methods Applied to Nuclear Science & Engineering. Nashville, TN, USA.
- Boyd, W., Shaner, S., Li, L., Forget, B., Smith, K., 2014. The OpenMOC Method of Characteristics Neutral Particle Transport Code. Annals of Nuclear Energy 68, 43–52.
- Boyd, W. R. D., 2016. Reactor Agnostic Multi-Group Cross Section Generation for Fine-Mesh Deterministic Neutron Transport Simulations. Ph.D. thesis, Massachusetts Institute of Technology (submitted).
- Cai, L., 2014. Condensation and Homogenization of Cross Sections for the Deterministic Transport Codes with Monte Carlo Method: Application to the GEN IV Fast Neutron Reactors. Ph.D. thesis, Université Paris Sud-Paris XI.
- Horelik, N., Herman, B., Forget, B., Smith, K., 2013. Benchmark for Evaluation and Validation of Reactor Simulations (BEAVRS), v1.0.1. In: Int. Conf. Math. and Comp. Methods Applied to Nuc. Sci. & Eng. Sun Valley, Idaho, USA.
- Lax, D., Boyd, W., Horelik, N., 2014. An Algorithm for Identifying Unique Regions in Constructive Solid Geometries. In: PHYSOR. Kyoto, Japan.
- Leppänen, J., 2013. Serpent – A Continuous-Energy Monte Carlo Reactor Physics Burnup Calculation Code. VTT Technical Research Centre of Finland.

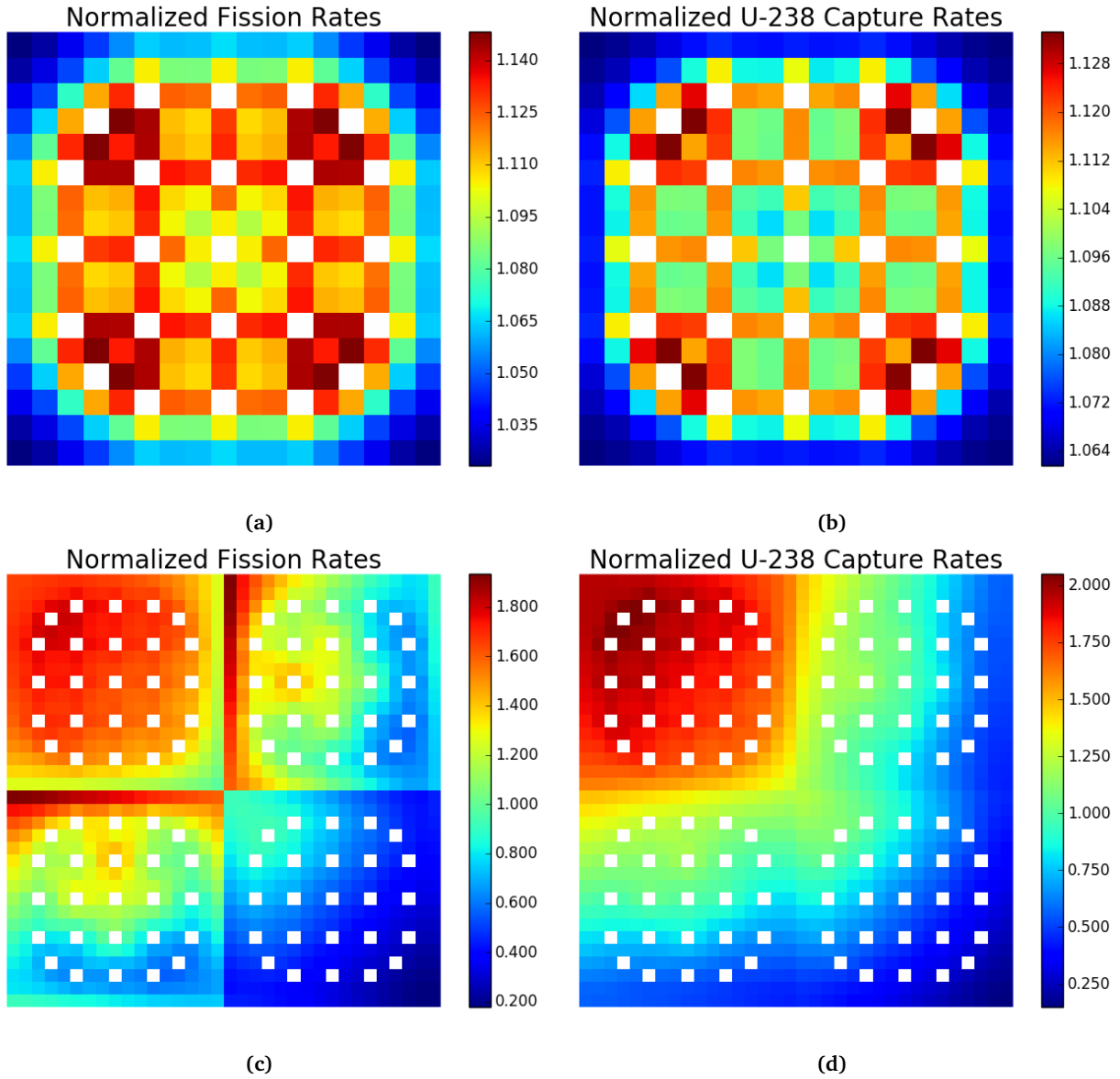


**Figure 3.** Reference OpenMC fission and U-238 capture rates for the assembly (a) – (b) and colorset (c) – (d) benchmarks.

- Nelson, A., 2014. Improved Convergence Rate of Multi-Group Scattering Moment Tallies for Monte Carlo Neutron Transport Codes. Ph.D. thesis, University of Michigan.
- Redmond, E. L., 1997. Multi-Group Cross Section Generation via Monte Carlo Methods. Ph.D. thesis, Massachusetts Institute of Technology.
- Rhodes, J., Smith, K., Lee, D., 2006. Casmo-5 development and applications. In: ANS Topical Meeting on Reactor Physics (PHYSOR). pp. 10–14.
- Romano, P K., Forget, B., 2013. The OpenMC Monte Carlo Particle Transport Code. Annals of Nuclear Energy 51, 274–281.
- X-5 Monte Carlo Team, 2003. MCNP-A General Monte Carlo N-Particle Transport Code, Version 5. , Los Alamos National Laboratory.

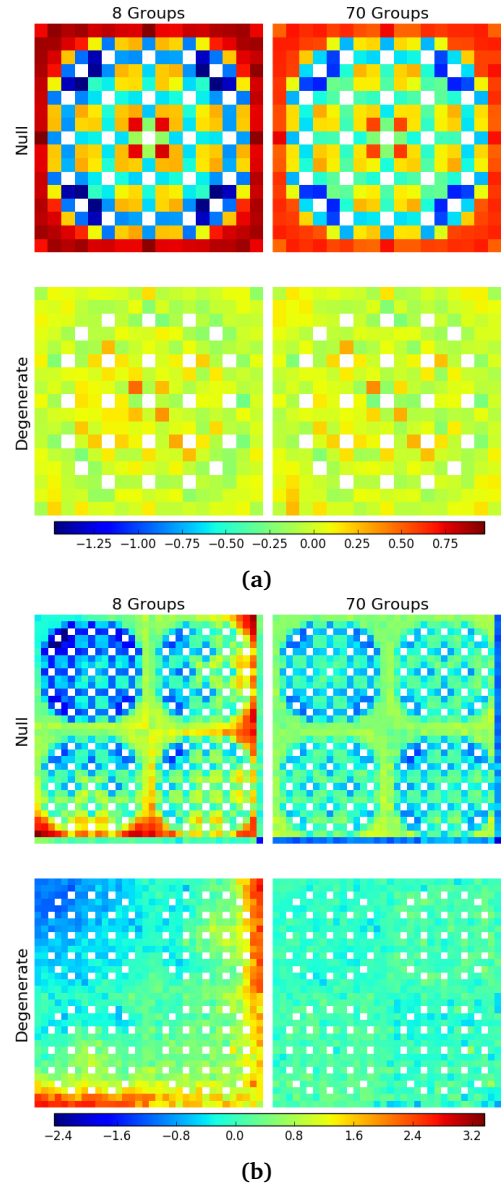
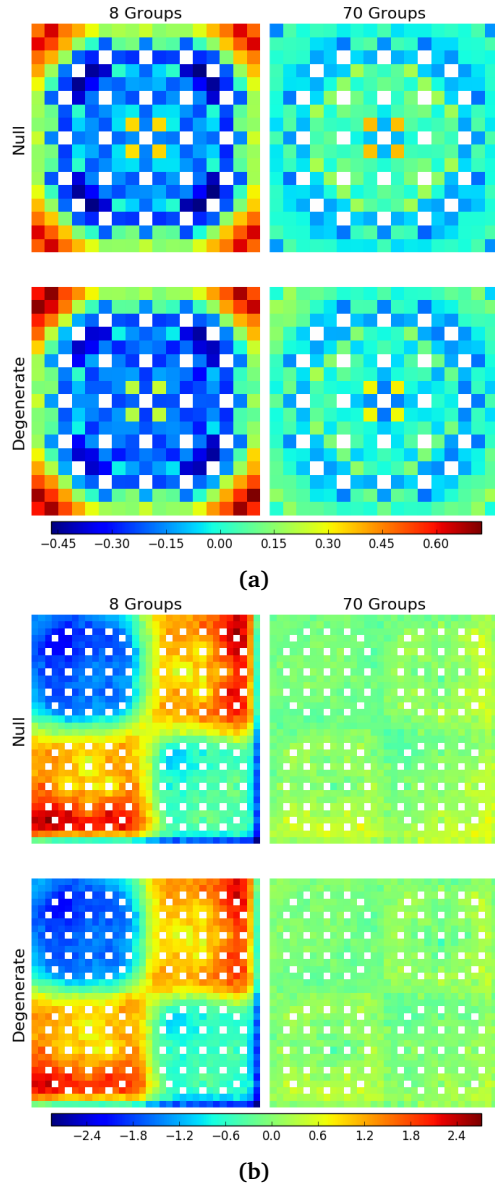


**Figure 4.** OpenMOC fission rate percent relative errors for the (a) assembly and (b) 2x2 colorset models.

**Figure 5.** OpenMOC U-238 capture rate percent relative errors for the (a) assembly and (b) 2x2 colorset models.